Correspondence to:
U. Lohmann,
ulrike.lohmann@env.ethz.ch

The influence of absorbed solar radiation by Saharan dust on hurricane genesis

Sebastian Bretl[1], Philipp Reutter[2], Christoph C. Raible[3], Sylvaine Ferrachat[1], Christina Schnadt Poberaj[1], Laura E. Revell[1], and Ulrike Lohmann[1]

[1]Institute of Atmospheric and Climate Sciences, ETH Zürich, Zürich, Switzerland, [2]Institute for Atmospheric Physics, Johannes Gutenberg University, Mainz, Germany, [3]Climate and Environmental Physics and Oeschger Centre for Climate Change Research, University of Bern, Bern, Switzerland

Abstract To date, the radiative impact of dust and the Saharan air layer (SAL) on North Atlantic hurricane activity is not yet known. According to previous studies, dust stabilizes the atmosphere due to absorption of solar radiation but thus shifts convection to regions more conducive for hurricane genesis. Here we analyze differences in hurricane genesis and frequency from ensemble sensitivity simulations with radiatively active and inactive dust in the aerosol-climate model ECHAM6-HAM. We investigate dust burden and other hurricane-related variables and determine their influence on disturbances which develop into hurricanes (developing disturbances, DDs) and those which do not (nondeveloping disturbances, NDDs). Dust and the SAL are found to potentially have both inhibiting and supporting influences on background conditions for hurricane genesis. A slight southward shift of DDs is determined when dust is active as well as a significant warming of the SAL, which leads to a strengthening of the vertical circulation associated with the SAL. The dust burden of DDs is smaller in active dust simulations compared to DDs in simulations with inactive dust, while NDDs contain more dust in active dust simulations. However, no significant influence of radiatively active dust on other variables in DDs and NDDs is found. Furthermore, no substantial change in the DD and NDD frequency due to the radiative effects of dust can be detected.

1. Introduction

Tropical cyclones (TCs) and the processes leading to their genesis have since long been a topic of interest in the scientific community. Since the 1950s, six prerequisites were identified as important for TC generation, e.g., *Ramage* [1959], *Lighthill et al.* [1994], *Gray* [1998], and *Tory and Frank* [2010]: (1) Ocean temperatures in the topmost 50 m exceeding 26.0–26.5°C; (2) A potentially unstable atmosphere; (3) A moist midtroposphere; (4) Latitudes more than 5° away from the equator; (5) An initial dynamic disturbance with sufficient convergence and vorticity, e.g., a tropical easterly wave; and (6) A low vertical shear of the horizontal winds.

Dust can potentially influence four of these criteria (numbers 1, 2, 3, and 6, as discussed below). In this regard the Sahara as the world's largest dust source [*Washington et al.*, 2003] is a key factor. In distinct outbreaks, the dry, warm, and dust-laden Saharan air layer (SAL) is elevated over West Africa and transports dust across the North Atlantic during the Northern Hemisphere summer months [*Carlson and Prospero*, 1972; *Prospero and Carlson*, 1981]. In total, about 25% of Saharan dust emissions are transported westward to the Atlantic [*d'Almeida*, 1986; *Shao et al.*, 2011].

To date, two main effects of aerosols on TCs have been studied: The microphysical effect, which examines how the aerosol particles act as cloud condensation nuclei (CCN) and ice nuclei, and the radiative/dynamic effect, which takes into account the effect of absorption and scattering of solar radiation by aerosol particles with possible subsequent implications on atmospheric dynamics. The concept of seeding TCs with aerosols to reduce their intensity was analyzed as part of the STORMFURY project [*Gentry and Hawkins*, 1970; *Willoughby et al.*, 1985]. *Cotton et al.* [2007] and *Zhang et al.* [2007, 2009] gave an overview of the simulated hurricane response to African dust. They proposed that seeding hurricanes with dust acting as CCN could reduce hurricane intensity. Besides CCN, giant CCN and ice nuclei potentially contribute to this mechanism [*DeMott et al.*, 2003; *van den Heever et al.*, 2006]. In a case study, *Khain et al.* [2010] showed that continental aerosols invigorate convection largely at the TC periphery, leading to TC weakening. Similar results were found by *Carrio and Cotton* [2011] in seeding during virtual aircraft flights. Although another case study

found an increase in low-level wind speed in the first 10 h after ingestion of CCN prior to a substantial weakening of wind speeds below the winds of a control run [*Krall and Cottom*, 2012], most studies found that additional CCN generally weaken TC intensity, e.g., *Rosenfeld et al.* [2011] and *Rosenfeld et al.* [2012].

While there seems to be a consensus on the microphysical impact of dust on TCs, it is controversial whether the radiative effects of dust and the SAL reduce or strengthen TC activity. Using Geostationary Operational Environmental Satellite split-window satellite imagery, *Dunion and Velden* [2004] identified SAL outbreaks and assigned reduced intensification of TCs to these SAL outbreaks. They attributed this to three mechanisms: an enhanced low-level temperature inversion triggered by the SAL, possibly inhibiting convection in weak African easterly waves (AEWs); dry air intrusion into the TC, which is associated with a reduction of convective available potential energy; and increased vertical wind shear induced by the SAL midlevel easterly jet. *Evan et al.* [2006] detected an inverse relationship of dust cover and North Atlantic TC activity by evaluating Advanced Very High Resolution Radiometer data for the years 1982–2005 but admitted that this relationship is not proof for a causal effect of dust controlling TC activity. *Lau and Kim* [2007a] assigned the reduced hurricane activity of 2006 compared to 2005 to the significantly lower sea surface temperatures (SSTs); 30–40% of the SST reduction was attributed to the radiative cooling effect of dust aerosols [*Lau and Kim*, 2007b]. In contrast to *Lau and Kim* [2007a], *Foltz and McPhaden* [2008] suggested that dust-induced changes in surface shortwave radiation played only a minor role in the cooling of the North Atlantic between 2005 and 2006. The reduced TC activity in 2007 with respect to 2005 was associated with further westward transport of the SAL [*Sun et al.*, 2008]. Therefore, except for conditions 4 and 5, dust could indeed influence the remaining four prerequisites for TC genesis.

However, recent studies affirming a negative impact of the SAL on hurricane activity [e.g., *Dunion and Velden*, 2004; *Lau and Kim*, 2007a] barely considered alternative causes of storm weakening or lack of intensification such as changes in vertical wind shear, ocean cooling induced by hurricanes, or weak convective activity not associated with the SAL. Hence, *Braun* [2010] claimed that these studies were largely built on limited evidence and some false assumptions and emphasized the African Easterly Jet (AEJ) as a source of energy for AEWs. AEWs are known to be conducive for hurricane formation [*Frank and Clark*, 1980; *Landsea*, 1993; *Frank and Roundy*, 2006] and for the transport of desert dust over the Atlantic [*Jones et al.*, 2003]. In fact, there are also a number of studies showing a supporting effect of the SAL on hurricane formation: Using the Global Atmospheric Research Program Atlantic Tropical Experiment [*Kuettner*, 1974], *Karyampudi and Carlson* [1988] claimed that SAL outbreaks are possibly necessary but at least important for the initialization of easterly wave disturbances. In case studies, an inhibiting effect of the SAL was found on Hurricane Andrew (1992), whereas enhancing effects were observed for Tropical Storm Ernesto (1994) and Hurricane Luis (1995) [*Karyampudi and Pierce*, 2002]. Furthermore, *Braun* [2010] noted that the frontogenetic properties of the warm SAL seem to facilitate an indirect vertical circulation enhancing convection and thus promoting storm development. He further mentioned that deep saturated ascent is confined to the region to the south where vertical shear associated with the AEJ is weak. However, this does not imply that the Intertropical Convergence Zone (ITCZ) is shifted to the south due to dust aerosols, it seems to be rather the opposite. *Reale et al.* [2011] emphasized that recent experiments with general circulation models show a northward shift of the Atlantic ITCZ caused by radiative effects of Saharan dust. In their quarter-degree simulations with 72 vertical levels, they found the AEJ to be displaced slightly northward during strong Saharan dust outbreaks. This is in agreement with *Wilcox et al.* [2010], who found a northward shift of the ITCZ during SAL dust outbreaks using satellite observations and atmospheric reanalysis data products, and a recent model study by *Woodage and Woodward* [2014]. Combining microphysical and radiative effects of anthropogenic aerosols, *Wang et al.* [2014] hypothesized that anthropogenic aerosols have an opposite effect to that of greenhouse gases and noted the importance of using microphysical radiative modules in atmospheric models for TC research.

Recently, *Reale et al.* [2014] used the assimilated aerosol optical depth from the Moderate Resolution Imaging Spectroradiometer for interactive aerosol modeling. They performed two sets of simulations with aerosol direct radiative effects (termed *active* dust hereafter) and without radiative effects (termed *inactive* dust hereafter) for 1 month in 2006 to determine the role of dust on the development of a TC and found that dust radiative effects cause the environment to be less conducive to TC development.

Here we use a similar approach with radiatively active and inactive dust but evaluate the influence of dust on hurricane genesis in the North Atlantic on a statistical basis. For this purpose, sensitivity simulations

Table 1. Radiative Effects of Dust and Usage of HAM in Different Versions of ECHAM6 Used in This Study

	Radiative Effects of Dust	Version of HAM
ECHAM6-dust	interactive (active dust)	simplified
ECHAM6-no-dust	none (inactive dust)	simplified
ECHAM6	climatological	not included

are performed with the general circulation model ECHAM6 [*Stevens et al.*, 2013] coupled to the aerosol module HAM [*Stier et al.*, 2005; *Zhang et al.*, 2012] in a simplified version. Two sets of ensemble sensitivity simulations are performed: One with radiatively active dust and one with inactive dust. Using seasonal ensemble means, we evaluate dust-induced mechanisms associated with the SAL as proposed by *Dunion and Velden* [2004] and *Braun* [2010]. A "box difference index" (BDI) [*Peng et al.*, 2012] is used to detect a possible influence of dust on hurricanes and to compare the importance of dust in hurricane genesis to other variables such as wind shear and vorticity. With this setup, we investigate which role Saharan dust plays during hurricane genesis when interacting with incoming solar radiation and how large its impact is. The mechanisms suggested by *Dunion and Velden* [2004] and *Braun* [2010] on the relationship between dust and hurricane intensity and genesis are tested in our sensitivity simulations.

2. Method

2.1. Model and Simulations

We use a simplified version of the aerosol-climate model ECHAM6-HAM [*Zhang et al.*, 2012; *Stevens et al.*, 2013] in a spectral resolution of T255 on a quadratic Gaussian grid (approximately $0.5° \times 0.5°$) with 31 σ pressure levels reaching up to 10 hPa and a one-moment microphysical cloud convection scheme. The horizontal resolution enables us to obtain a realistic number of storms, but intense hurricanes exceeding category 1 on the Saffir/Simpson hurricane scale [*Simpson and Saffir*, 1974], using minimum sea level pressure as categorization criterion, are hardly simulated [*Murakami and Sugi*, 2010; *Raible et al.*, 2012; *Murakami et al.*, 2012; *Strachan et al.*, 2013]. In the model, which is simplified for this study due to computational constraints, dust is the only interactive aerosol. All remaining aerosol species use climatological values.

The particle size distribution of interactive aerosols in HAM is represented by a superposition of log normal modes, where dust is confined to the accumulation and coarse modes. Dust emissions in HAM are governed by wind speed and hydrological parameters [*Tegen et al.*, 2002], while removal processes include sedimentation and dry and wet deposition [*Stier et al.*, 2005]. In the standard ECHAM6-HAM model, wet deposition of dust particles includes coating and coagulation processes with sulfates. In our simplified ECHAM6-HAM sulfate is not calculated interactively and thus does not interact with dust. Therefore, the scavenging parameters, which govern removal processes of dust particles, are adjusted to adequately simulate North Atlantic dust concentrations. The complex refractive index of dust in HAM is $1.52 + 1.1\times10^{-3}\ i$ at 550 nm, following *Kinne et al.* [2003]. Shallow convection in ECHAM6 is treated following the Tiedtke scheme [*Tiedtke*, 1989], while deep convection includes changes introduced by *Nordeng* [1994].

Table 2. Number of Storm Tracks in Observations and Simulations of 2005 and 2006, Nudged Toward ERA-Interim Reanalysis Data (June–November)[a]

	Observed	$\zeta : 3 \times 10^{-5}$	$\zeta : 5 \times 10^{-5}$	$\zeta : 10 \times 10^{-5}$
2005				
Hurricanes	13	13	13	12
Tropical storms	11	2	2	1
Additional tracks	–	9	4	1
2006				
Hurricanes	5	4	4	4
Tropical storms	5	3	3	1
Additional tracks	–	6	3	0

[a]The column "ζ" denotes the vorticity threshold of the simulations (s^{-1}). "Tropical storms" shows only storms which did not reach hurricane intensity. "Additional tracks" refer to detected systems that were not categorized as a hurricane or tropical storm by the National Hurricane Center (NHC).

Table 3. Numbers of the On-Average-Detected North Atlantic Storms in NHC Observations and Ensemble Simulations (ECHAM6-Dust and ECHAM6-No-Dust) Between June and September[a]

	Tropical Storms	Hurricanes	Major Hurricanes
Observations (1851–2010)	6.5	4.0	1.5
Observations (1981–2010)	9.0	4.7	2.2
Observations (2005)	17	10	5
Simulations (20 × 2005)	7.6	0.9	0.1

[a]"Tropical storms" includes all named tropical systems (simulations: all tracks), "Hurricanes" all storms reaching hurricane intensity, "Major Hurricanes" all hurricanes of categories 3–5.

The simulated atmospheric state of ECHAM6 was thoroughly evaluated with ERA-Interim reanalyses [*Stevens et al.*, 2013].

SSTs are prescribed as climatological monthly averages. This implies that the direct radiative effects of dust are simulated with a noninteractive ocean surface. Previous studies determined some dust-induced decrease of North Atlantic SST [*Lau and Kim*, 2007a, 2007b; *Martínez Avellaneda et al.*, 2010], but it may be small [*Foltz and McPhaden*, 2008]. With our approach of fixed SSTs, we try to isolate the atmospheric responses of the radiative effects of dust as proposed by *Dunion and Velden* [2004].

Two sets of simulations are performed: The first set consists of 10 free ensemble simulations of the year 2005 with dust being radiatively active (ECHAM6-Dust). Differences in initial conditions are obtained by minimal perturbations of stratospheric horizontal diffusion [*Vamborg et al.*, 2014]. The second set of simulations uses the same setup, but with the interaction between dust and radiation switched off (ECHAM6-no-dust). Table 1 shows the types of ECHAM6 used in this study, if the simplified HAM is used and how radiative effects of dust are treated in the different simulations. The year 2005 is selected because its North Atlantic hurricane season was the most active ever recorded [*Beven et al.*, 2008], with SSTs more than 1°C above the long-term mean (1950–2000) in the main development region [*Sun et al.*, 2008]. With the above average SSTs of 2005 we expect a larger number of hurricanes than we would obtain for other years, generating a larger database to detect possible changes in hurricane activity between ECHAM6-Dust and ECHAM6-no-dust simulations. Because we use prescribed SSTs, only the direct influence of dust leading to a warming, drying, and a subsequent stabilization of the atmosphere are considered in this study. AEWs peak during the summer months; therefore, only the first 4 months of the North Atlantic hurricane season, June–September, are taken into account in our study. For the analysis we use 6-hourly model output data. The microphysical influence of dust aerosols acting as cloud condensation nuclei or ice nuclei and thus modulating hurricane activity [e.g., *Zhang et al.*, 2007; *Rosenfeld et al.*, 2011, 2012] is not included in our model setup.

2.2. Seasonal Differences Between ECHAM6-Dust and ECHAM6-No-Dust Simulations

Dunion and Velden [2004] named three mechanisms which explain the inhibiting effect of dust and the SAL on hurricane intensity (section 1). We examine these three mechanisms also for tropical cyclogenesis in our model by looking at possible changes in seasonal ensemble averages (June–September) in temperature, relative humidity, and wind shear between ECHAM6-Dust and ECHAM6-no-Dust simulations. *Braun* [2010] described a vertical circulation associated with the AEJ, which confines convection to the south where vertical wind shear is weak. Hence, we also investigate dust-induced changes in seasonal ensemble averages of zonal and meridional wind and 700 hPa vertical velocity.

2.3. Tracking

We track disturbances which developed into a TC (developing disturbances, DDs) and those which did not develop (nondeveloping disturbances, NDDs). The DDs are tracked using the detection and tracking criteria from *Kleppek et al.* [2008] and *Raible et al.* [2012]: A local minimum in sea level pressure (SLP), relative vorticity at 850 hPa exceeding 5×10^{-5} s^{-1}, vertical wind shear between 200 and 850 hPa below 15 m s^{-1} and a minimum lifetime criterion. The threshold value of wind shear is set to ≤15 m s^{-1} instead of the original ≤10 m s^{-1} to detect storms at an earlier stage. The vorticity threshold is tested in simulations of the years 2005 and 2006, nudged to ERA-Interim reanalyses (Table 2). Although other studies used also higher
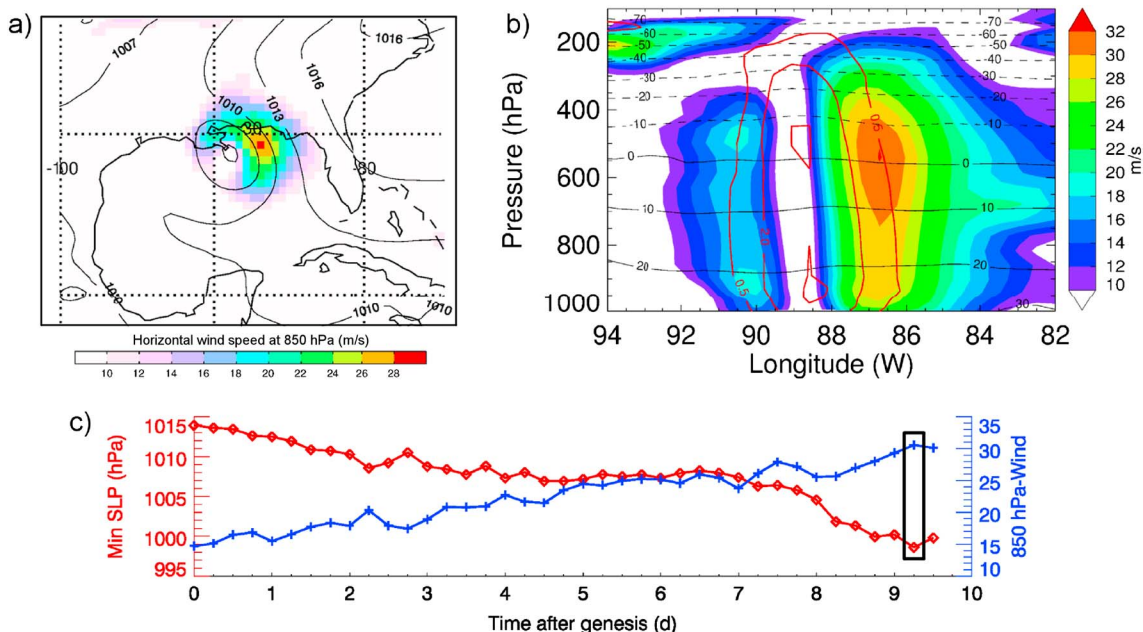
Figure 1. Depiction of the most intense storm within our 20 ensemble simulations originating in our defined region between 20°W and 50°W. (a) Wind speed at 850 hPa and sea level pressure during its most intense phase, (b) Zonal cross section of the storm with horizontal wind speed (shading), temperature in °C (black lines), and vorticity in 0.5, 2, and 4×10^{-4} s^{-1} (red lines) during the same time step as in Figure 1a, (c) Evolution of minimum SLP and 850 hPa wind speed of the storm during its whole lifetime. The black box shows the time of the storm in Figures 1a and 1b, 12 h after reaching its maximum intensity, it was not detected any more.

vorticity threshold values [*Bengtsson et al.*, 2007a, 2007b], 5×10^{-5} s^{-1} is the optimal threshold tested to detect and track hurricanes in our simulations. An additional SST criterion is added, tracking only storms over areas with SSTs ≥25°C on their initial time step [*Dare and McBride*, 2011]. We furthermore reduced the minimum lifetime criterion to ≥18 h. This threshold is a bit lower than that in comparable studies [*Bengtsson et al.*, 2007b; *Kleppek et al.*, 2008; *Murakami et al.*, 2013], but is required to counteract the too low number of DDs in the North Atlantic in ECHAM6 with minimum lifetimes, e.g., 24 or 36 h.

To detect NDDs, the tracking algorithm of *Kleppek et al.* [2008] is modified. NDDs are tracked as local maxima of 850-hPa relative vorticity. Three criteria, similar to the NDD criteria of *Murakami et al.* [2013], need to be fulfilled with this new vorticity tracking method: (1) The magnitude of the maximum 850 hPa vorticity needs to exceed 4×10^{-5} s^{-1}; (2) To obtain NDDs with a certain size, the averaged 850 hPa vorticity in a 5° × 5° box around its center needs to exceed 2.5×10^{-5} s^{-1}; (3) The minimum lifetime of a detected system is 66 h. The latter is just slightly below the NDD lifetime criterion of 72 h used by *Peng et al.* [2012]. With these settings we tried to achieve a ratio of roughly 1 to 2 between DDs and NDDs, which
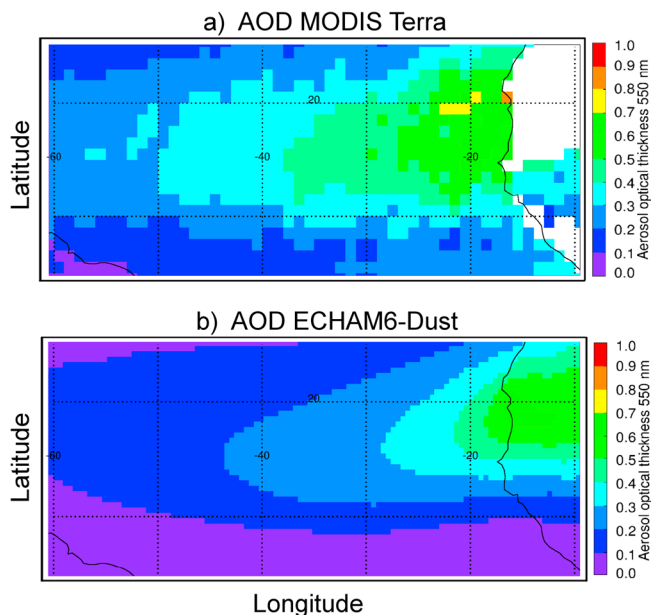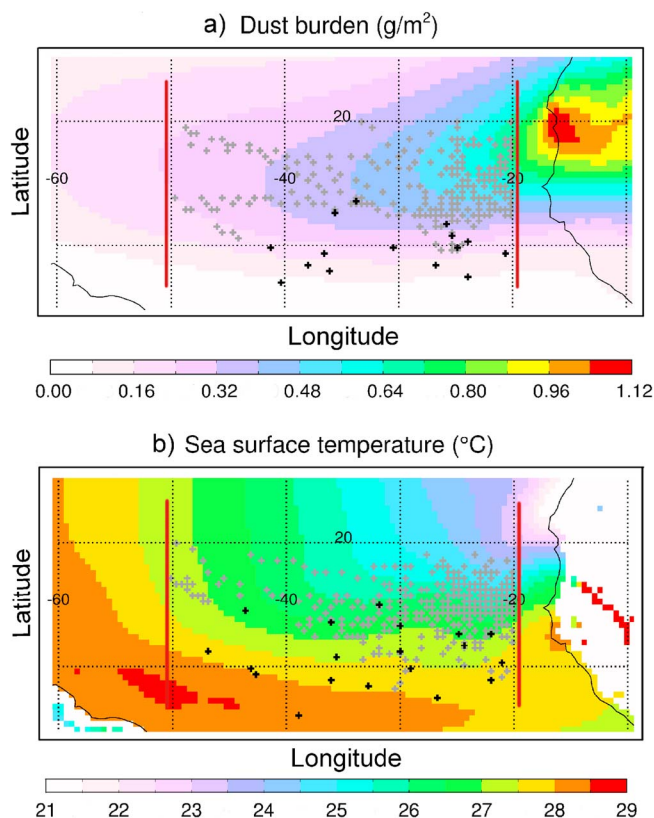

Figure 2. June to September (2005) mean aerosol optical depth at 550 nm with (a) MODIS Terra observations and (b) Average of 10 ensemble simulations with ECHAM6-Dust.

Figure 3. June to September mean of (a) dust burden and (b) SST in the simulations with ECHAM6-Dust. Black crosses show the DDs in ECHAM6-Dust (Figure 3a) and ECHAM6-no-dust (Figure 3b) 24 h prior to detection. Grey crosses denote NDDs every 6 h in ECHAM6-Dust (Figure 3a) and ECHAM6-no-dust (Figure 3b). Dark red lines denote our defined region between 20°W and 50°W.

is similar to the ratios found in *Peng et al.* [2012] and *Murakami et al.* [2013].

2.4. Composites and Box Difference Indices

The BDI is an index designed to determine the ability of a given variable to control TC genesis [*Peng et al.*, 2012]. For a given box size the BDI is defined as

$$BDI = \frac{M_{DD} - M_{NDD}}{\sigma_{DD} + \sigma_{NDD}}$$

where the indices DD and NDD depict composites of DDs and NDDs, respectively. M and σ denote the mean and standard deviation of the respective composites of a variable of interest. The sign of the BDI indicates a correlation (+) or anticorrelation (−).

Using this technique, various variables can be compared with each other in terms of their importance as controlling variables for TCs. In observational studies, *Peng et al.* [2012] used the BDI to identify controlling parameters for hurricane genesis in the North Atlantic, while *Fu et al.* [2012] examined TCs in the western North Pacific. *Murakami et al.* [2013] applied the BDI on TC genesis in a global warming scenario

compared to a present-day climate. In this study, the BDI is also applied on dust. As the average dust loading over the North Atlantic significantly decreases toward the west, we only consider disturbances between 20°W and 50°W. This excludes disturbances in regions with dust burdens too low to have an impact on hurricane genesis.

In this study composites are made for DDs and NDDs in a 5° × 5° box in longitude and latitude. The box moves with the disturbances so that the storm center is always in the middle. The NDD composites consist of 6-hourly output of an NDD once it is located inside our defined region between 20°W and 50°W. With this,
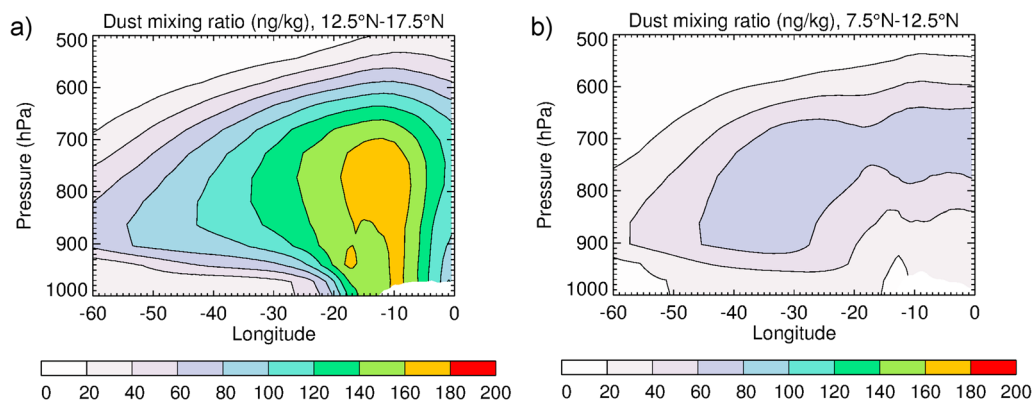

Figure 4. Ensemble mean dust mixing ratio of the ECHAM6-Dust simulations (June–September) meridionally averaged between (a) 12.5°N–17.5°N and (b) 7.5°N–12.5°N.
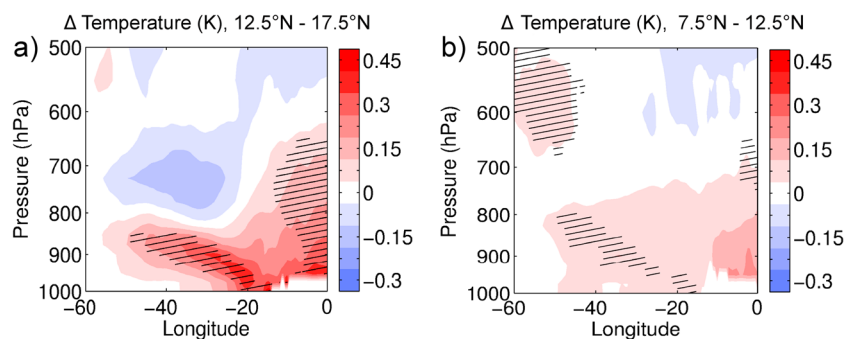
Figure 5. Ensemble-mean temperature differences between ECHAM6-Dust and ECHAM6-no-dust simulations (June–September) meridionally averaged between (a) 12.5°N–17.5°N and (b) 7.5°N–12.5°N. Lined shading denotes statistical significant changes at the 5% level (two-sided t test).

we use characteristic conditions of NDDs which inhibit development during their whole lifetime. Detected DDs are traced back according to their 850 hPa relative vorticity centers. For the DD composites, including time steps at the stage of a TC would lead to an ordinary comparison between hurricanes and weaker tropical storms, losing the crucial development stage of hurricanes. However, the aim is to examine DDs at a stage where they do not yet show hurricane-like features but are in a transition phase when environmental conditions become more conducive for hurricane development. For this reason, we present only results for the time step 24 h prior to their detection as TCs.

In our ensemble sensitivity simulations the following variables are investigated: dust burden, SST, relative humidity in typical SAL heights of 850 and 700 hPa, maximum relative vorticity in 700 hPa, and vertical wind shear between 200 and 850 hPa. As the 850 hPa level is close to the bottom of the SAL, low- to middle-level winds may be underestimated [*Dunion and Velden*, 2004]. Hence, our lower tropospheric winds in 850 hPa denote the mean of the 700–925 hPa layer. As mentioned above, SST, vorticity, and wind shear are known to be decisive factors for TC formation.

3. Results

3.1. Limitations Due to Spatial Resolution
The simulation of realistic tropical cyclones requires an adequate spatial resolution. While to date the influence of vertical resolution on TCs is hardly discussed in literature, the effect of horizontal resolution has been subject to several studies, e.g., *Bengtsson et al.* [2007b];, *Murakami and Sugi* [2010], and *Strachan et al.* [2013]. Our horizontal resolution of around 52 km enables us to realistically simulate the frequency of tropical storms [*Strachan et al.*, 2013] but not with the observed intensity (Table 3). Within 20 ensemble simulations (June–September), only two intense hurricanes are generated with minimum SLPs of 948 and 962 hPa, located in the Gulf of Mexico. All remaining storms in the North Atlantic did not undershoot 980 hPa. The most intense storm forming in our defined region between 20°W and 50°W only reached 1000 hPa (Figure 1). Furthermore, the maximum wind is found in a height of 550 hPa, which is in much higher altitudes than in reality [*Nolan et al.*, 2009]. Two time steps after the minimum SLP was obtained; the
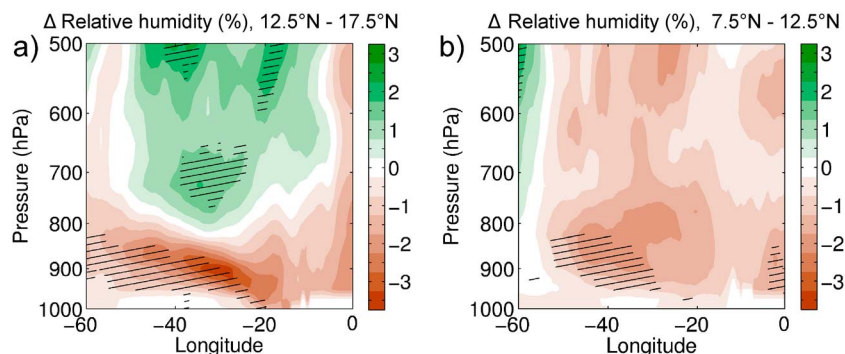

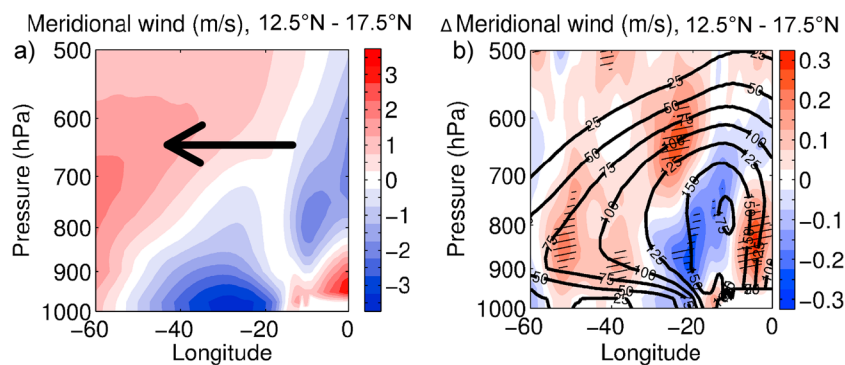**Figure 6.** As in Figure 5 but for relative humidity.

Figure 7. Ensemble mean meridional wind between 12.5°N and 17.5°N (June–September): (a) Simulations with ECHAM6-no-dust and (b) difference between ECHAM6-Dust and ECHAM6-no-dust simulations. Thick contours in Figure 7b denote dust mixing ratio in ECHAM6-Dust, intervals of 25 ng kg^{-1}. The black arrow depicts the schematic position of the African easterly jet; lined shading denotes statistical significant changes at the 5% level (two-sided t test).

storm was not detected any more due to a slight increase in wind shear. In a recent study, *Lim et al.* [2014] suggested that a resolution of 0.5° is not suitable to investigate TCs in a global framework, but a grid of 0.25° or smaller is needed. *Zarzycki and Jablonowski* [2014] used a 1° resolution for simulations with the Community Atmosphere Model and embedded a 0.25° grid for the region around a TC once it is detected during the Atlantic hurricane season (June–November). They found TC count, spatial distribution and tracks to resemble observations, with intensities of up to 80 m s^{-1}. The low intensity of our hurricanes is a limitation of our results that needs to be kept in mind.

3.2. Simulated and Observed Dust

For validation of atmospheric dust loadings, the mean aerosol optical depth (AOD) is compared to observations. For the simulations, we took mean values of the 10 free ensemble simulations of 2005 with ECHAM6-Dust. AOD observations were obtained using the MODerate resolution Imaging Spectroradiometer (MODIS) on the Terra spacecraft [*Savtchenko et al.*, 2004]. For both simulations and observational data, average values of June–September 2005 were taken. The model was not sampled along the Terra track. Hence, the simulation mean consists of all model time steps, while MODIS observations take into account solely data points of Terra overflights. In ECHAM6-Dust simulations the AOD is slightly lower than in observations (Figure 2). As simulated dust emissions are highly sensitive to wind speed and aerosol removal processes, differences are likely due to them. The simulated decrease in AOD toward the west is similar to what MODIS observed. Hence, the adjustment of our scavenging parameters for wet deposition in our simplified ECHAM6-HAM seems justified. Further comparisons of simulated AOD and dust concentrations in ECHAM6-HAM to observations were given by *Stanelle et al.* [2014].

3.3. Mean Background Climate During DDs and NDDs

NDDs in ECHAM6-Dust and ECHAM6-no-dust simulations are located mainly between 12.5°N and 17.5°N (hereafter termed the NDD region), while DDs are located primarily between 7.5°N and 12.5°N (hereafter termed the DD region, see Figure 3). For the discussion of Figures 4–7, we define the SAL as regions where
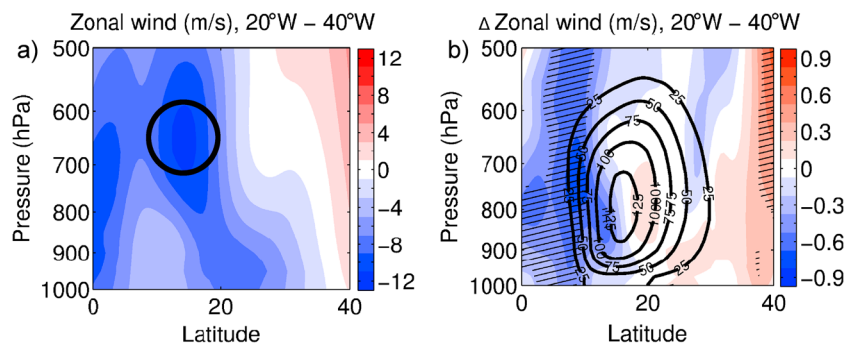

Figure 8. As in Figure 7 but for zonal wind between 20°W and 40°W (June–September). The black circle depicts the schematic position of the African easterly jet in our simulation.
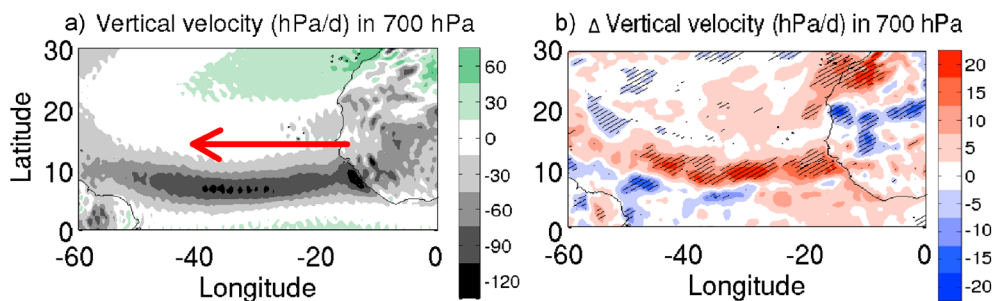
Figure 9. Ensemble mean vertical velocity in 700 hPa (June–September), (a) ECHAM6-no-dust and (b) difference between ECHAM6-Dust and ECHAM6-no-dust simulations. The red arrow depicts the schematic position of the African easterly jet in our simulations, lined shading denotes statistical significant changes at the 5% level (two-sided *t* test).

the dust mixing ratio exceeds 20 ng kg^{-1}, averaged over 5° in latitude. The results do not depend crucially on this threshold. The main NDD region coincides with the main part of the SAL over the tropical North Atlantic. The SAL extends up to around 500 hPa at 20°W (Figure 4a) with peak dust concentrations between 800 and 900 hPa. The SAL in ECHAM6 becomes thinner to the west with the top height decreasing and base slightly increasing resembling the observations of *Prospero and Carlson* [1981]. Due to absorption of solar radiation by dust, the atmosphere shows a statistically significant warming in the lower part of the SAL (roughly 950–850 hPa, Figure 5a) between 20°W and 50°W, and averaged over 12.5°N–17.5°N when comparing ECHAM6-Dust with ECHAM6-no-dust simulations. This warming increases the stability in this region and subsequently reduces the probability of storms forming during dust outbreaks. The same warming pattern is found by *Reale et al.* [2014] and is probably caused by the decrease in dust concentration with altitude and the dependence of absorption on particle size as larger dust particles absorb more solar radiation than smaller ones [*Tegen and Lacis*, 1996; *Helmert et al.*, 2007]. The settling of larger particles leaves mainly smaller particles within the upper parts of the SAL, which are too small to cause a warming. However, the warming depends on the dust particle size distribution, optical properties and removal parameterization in the model. On the contrary, the upper part of the SAL shows a slight cooling. We hypothesize the conservation of radiative equilibrium to be responsible for this cooling. However, as in comparable studies [*Wong et al.*, 2009; *Wilcox et al.*, 2010; *Reale et al.*, 2014] the exact mechanism of the cooling above the dust-induced warming could not be determined. Concomitant with the increase in temperature, the relative humidity shows a significant decrease within the lower SAL (Figure 6a).

In the main DD region (Figure 4b) in lower latitudes, dust concentrations are not as high as in the NDD region between 12.5°N and 17.5°N. Hence, the warming is smaller (Figure 5b) but also reaches slightly higher altitudes than in the higher latitudes of the NDD region with only a few areas showing a statistically significant warming. Nevertheless, this small warming could still inhibit convection when dust is radiatively active because the atmosphere is also slightly drier than in ECHAM6-Dust simulations (Figure 6b). However, dust concentrations in the DD region are lower than in the NDD region. Thus, one cannot attribute dust the same impact in the DD region compared to the NDD region. Neglecting other factors as SST and vertical
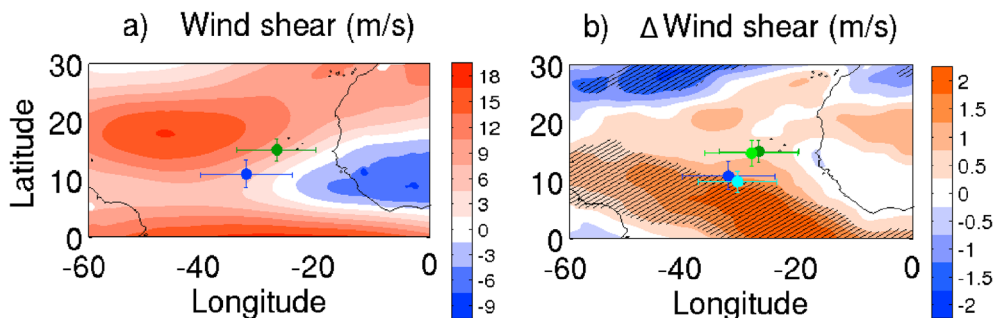

Figure 10. As in Figure 9 but for vertical wind shear between 200 and 850 hPa. (a) The dark blue dot depicts the average location of DDs in ECHAM6-no-dust, the dark green dot for NDDs, both with corresponding standard deviations. (b) Dark-blue and green dots as in Figure 10a, light-blue dot shows the average location of DDs in ECHAM6-Dust, light-green dot for NDDs.

Table 4. Numbers of the On-Average Detected Disturbances in Both Sets of Simulations and Corresponding Standard Deviations Between June and September[a]

	# Developing	# Nondeveloping
ECHAM6-dust	1.5 ± 1.4	3.3 ± 1.6
ECHAM6-no-dust	1.9 ± 1.4	4.2 ± 2.0

[a]Only disturbances within the region between 20°W and 50°W were taken into account.

wind shear which are known to have a large influence on hurricane genesis [*Dare and McBride*, 2011; *Molinari et al.*, 2004], the potential influence of dust seems to be larger in the NDD region than in the DD region.

As seen before, the variations in temperature between ECHAM6-Dust and ECHAM6-no-dust simulations cause a more stable low-level SAL at 12.5°N–17.5°N in ECHAM6-Dust simulations which subsequently cause differences in air motions. To illustrate this the meridional wind averaged over the NDD region shows a low-level southward flow between approximately 20°W and 40°W, while midlevels reveal northward flow (Figure 7a). This is in agreement with a vertical circulation associated with the SAL previously mentioned by *Braun* [2010]. This vertical circulation indicates southward flow below the AEJ and northward flow above with upward vertical motions on its southern edge and sinking on its northern edge. The dust-induced warming in the ECHAM6-Dust simulations causes both statistically significant increases in low-level southward and midlevel northward flows between 15°W and 30°W (Figure 7b), intensifying the meridional wind compared with ECHAM6-no-dust simulations. This is accompanied by a statistically significant increase of the westward flow of the AEJ south of the main dust region within the North Atlantic SAL and a slight decrease of this flow to the north (Figure 8).

Due to the increase in low-level southward meridional wind, convective regions are partly deflected. The vertical velocity ω in the ECHAM6-no-dust simulations shows a broad region with upward motions around 10°N (Figure 9a), depicting the ITCZ. Although there are statistically significant changes in upward vertical velocity which result in a southward shift of convection (Figure 9b), these changes are rather small. This shift is opposite to both observational [*Wilcox et al.*, 2010] and modeling studies [*Reale et al.*, 2011; *Woodage and Woodward*, 2014]; hence, it may be rather an artifact of our model resolution than an effect of dust aerosols. Vertical shear of zonal winds decreases toward the south between approximately 10°N and 18°N (Figure 10a), supporting hurricane genesis in lower latitudes. However, the vertical wind shear is higher in the tropical North Atlantic in ECHAM6-Dust simulations (Figure 10b). A moderate wind shear of up to 10 m s^{-1} is suggested to support TC genesis [*Bracken and Bosart*, 2000; *Molinari et al.*, 2004]. Thus, it depends on the magnitude of the background wind shear whether the dust-induced increase in wind shear lowers or raises the potential of hurricane genesis.

3.4. Frequency of Disturbances

Between 20°W and 50°W during June to September 2005, three tropical depressions were observed which developed into a hurricane. Fostered by the above average SSTs in the North Atlantic main development region (10°N–20°N, 20°W–80°W, *Sun et al.* [2008]), this is higher than the long-term average of the National Hurricane Center HURDAT database (1851–2009) of 1.3 hurricanes per season (June–September) in this region. A nonsignificant change in the frequency of DDs is found between ECHAM6-no-dust and ECHAM6-Dust simulations (1.9 versus 1.5 per season, Table 4). Compared to the observations of 2005, we underestimate the number of hurricanes/developing disturbances per season in ECHAM6-Dust and ECHAM6-no-dust simulations. The underestimation of hurricanes in the North Atlantic was also previously found for ECHAM5 [*Bengtsson et al.*, 2007a].

However, the frequency of DDs strongly depends on the lifetime criterion of the tracking algorithm. With 24 instead of 18 h as the minimum lifetime, an increase in frequency is found between ECHAM6-no-dust and ECHAM6-Dust simulations (1.0 versus 1.4 per season), while with 6 and 36 h we simulate a similar frequency of DDs. Hence, we cannot determine a robust dependence of DD frequency on the radiative properties of dust.

The number of NDDs between 20°W and 50°W per season is 4.2 for ECHAM6-no-dust and 3.3 for ECHAM6-Dust. This represents a

Table 5. Average Locations of DDs and NDDs in Both Sets of Simulations and Corresponding Standard Deviations

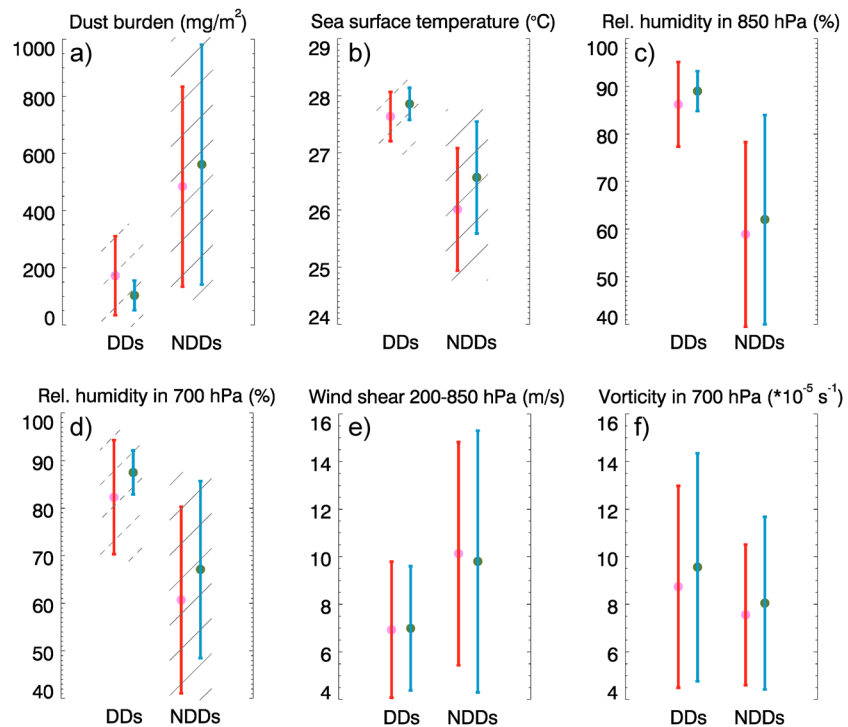|	ECHAM6-Dust	ECHAM6-No-Dust
Longitudes (DDs)	−30.9° ± 6.8°	−32.5° ± 8.0°
Longitudes (NDDs)	−28.5° ± 8.1°	−27.2° ± 6.9°
Latitudes (DDs)	9.8° ± 1.8°	10.8° ± 2.4°
Latitudes (NDDs)	14.7° ± 2.2°	15.0° ± 1.9°

Figure 11. Composites of variables for DDs and NDDs for a 5° × 5° box. Red dots show values for the simulations with ECHAM6-no-dust, blue dots for ECHAM6-Dust. Error bars indicate 1 standard deviation in each case. Straight diagonal shading denotes statistical significant changes between ECHAM6-no-dust and ECHAM6-Dust at the 5% level and dashed diagonal shading at the 10% level (two-sided *t* test).

decrease of around 25%, which is largely independent of the lifetime of the NDDs, but this decrease is not statistically significant.

3.5. Composites

DDs and NDDs in ECHAM6-Dust (Figure 3a) and ECHAM6-no-dust (Figure 3b) are characterized with a composite analysis of key variables for hurricane development. For this purpose, changes of the mean values between ECHAM6-no-dust and ECHAM6-Dust simulations are determined. Note that the DDs are located 4°–5° southward of the NDDs (Table 5). For most variables, differences between DDs and NDDs are therefore primarily due to different locations. This includes, e.g., SST, which increases considerably between 10°N and 20°N when going from North to South, while wind shear shows a decrease. In addition, dust concentrations decrease substantially between main NDD and DD regions.

In ECHAM6-no-dust, the mean dust burden for the DDs is around 170 mg m^{-2}; this amount triples for the NDDs (Figure 11a). The average dust burden close to the West African coastline at around 15°N to 18°N decreases rapidly westward and southward (Figure 3a). Therefore, a lower dust burden in DDs compared with NDDs is accompanied by warmer SSTs (Figure 3b). The SSTs are 1.5°C higher for DDs than for NDDs (Figure 11b). Background relative humidity (RH) between 12.5°N and 17.5°N (Figure 6a) shows an opposite development between ECHAM6-no-dust and ECHAM6-Dust in low level and midlevel; hence, composites are evaluated for two levels (Figures 11c and 11d). At 850 (700) hPa, the mean RH is 86% (82%) for the DDs and 59% (61%) for the NDDs. This is consistent with the background mean RH, which decreases between 850 and 700 hPa in the main DD region between 7.5°N and 12.5°N but partly increases between 12.5°N and 17.5°N (not shown). Vertical shear in the eastern tropical North Atlantic decreases toward the south; hence, mean vertical shear between 200 and 850 hPa is 7 m s^{-1} for DDs and around 10 m s^{-1} for NDDs (Figure 11e). The maximum 700 hPa relative vorticity is slightly lower for NDDs than for DDs (7.6 versus 8.7 s^{-1}, Figure 11f).

In ECHAM6-Dust, developing disturbances are located 1° southward of the DDs in ECHAM6-no-dust (Table 5). This southward shift matches the southward shift in convection mentioned in section 3.3 but is
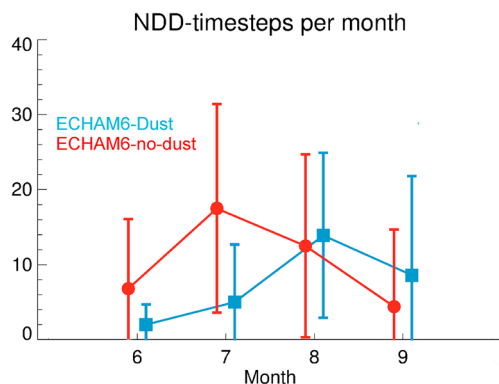
Figure 12. Number of NDD time steps per month and simulation within 20°W–50°W. Standard deviations are omitted below 0.

not statistically significant. While NDDs are only deflected 0.3° to the south, the southward shift of DDs has implications on composite averages. Between ECHAM6-no-dust and ECHAM6-Dust the mean dust burden decreases in DDs with changes being significant at the 10% level (two-sided t test). For NDDs, dust burden is significantly increased at the 5% level. As the location of the boxes around the disturbances varies from case to case, different composite values for SSTs are possible despite the fact that we use fixed SSTs. The mean SST of the composites is 0.2°C higher at the 10% significance level due to the southward shift of the DDs in ECHAM6-Dust. For NDDs, mean SSTs are larger by 0.5°C with significance at the 5% level. The reason for this is the temporal displacement of the NDDs. In our

defined region, SSTs rise between June and September, but the majority of NDD time steps which contribute to the BDI occur earlier in ECHAM6-no-dust than in the ECHAM6-Dust simulations (Figure 12). Hence, NDDs in ECHAM6-no-dust have lower SSTs than those in ECHAM6-Dust. As monthly mean locations between ECHAM6-no-dust and ECHAM6-Dust simulations are about the same, on-average NDDs in ECHAM6-Dust need warmer waters to compensate for the increased stability in these simulations. Similar results are found for the mean relative humidity at 700 and 850 hPa. While there is an increase in mean relative humidity in DDs due to the southward shift of DDs in ECHAM6-Dust, the increase in humidity of NDDs is caused by the temporal displacement of the NDDs as described above. Changes in humidity at 700 hPa are significant at the 5% (NDDs) and 10% (DDs) levels of confidence, but no statistical significant changes can be identified for 850 hPa. Mean vertical shear and maximum relative vorticity show only minor variations between ECHAM6-no-dust and ECHAM6-Dust simulations with no statistical significance.

3.6. BDIs

For determining the influence of dust on hurricane genesis we investigate differences in BDIs between ECHAM6-no-dust and ECHAM6-Dust. To quantify the differences in the DD and NDD composite means, the BDI is calculated for five variables for the 5° × 5° box (Figure 13). For the dust burden, the BDI varies only slightly between ECHAM6-no-dust and ECHAM6-Dust (−0.51 to −0.57). This indicates that the presence of dust in and around disturbances does not vary substantially when dust is radiatively active or inactive. For SST, the BDI decreases slightly from 1.09 to 1.02.

Relative humidity shows an increase in BDI between ECHAM6-no-dust and ECHAM6-Dust simulations from 0.68 to 0.88 at 700 hPa and from 0.87 to 1.03 at 850 hPa. These increases are both caused by the further southward located DDs in ECHAM6-Dust. The standard deviations of these DDs are smaller than in ECHAM6-no-dust. Due to the only minor and nonsignificant changes in wind shear in the composite means, vertical shear between 200 and 850 hPa reveals only small differences in BDIs of −0.36 to −0.41.
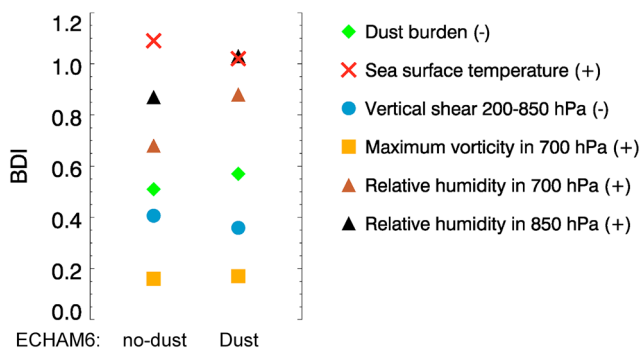

Figure 13. BDIs of evaluated variables for the 5° × 5° box for simulations with ECHAM6-no-dust and ECHAM6-Dust. The plus and minus symbols denote the sign of the variable's BDI.

The BDI of the maximum vorticity in 700 hPa remains almost constant between ECHAM6-no-dust (0.16) and ECHAM6-Dust (0.17).

Generally, the BDIs of all variables do not differ substantially between ECHAM6-no-dust and ECHAM6-Dust simulations. However, one has to keep in mind that only direct aerosol effects are considered. According to our results, controlling parameters for hurricane genesis do not depend crucially on dust. As the BDIs hardly differ between ECHAM6-no-dust and ECHAM6-Dust, the presence

of dust in and around the disturbances is not a sufficient criterion to determine an influence of dust on hurricane genesis. With our model we can reproduce the results obtained by *Peng et al.* [2012] who found that thermodynamic variables are the more important controlling parameters than dynamic variables.

4. Discussion and Conclusions

Previous studies showed inhibiting impacts of dust and the SAL on hurricane activity [*Dunion and Velden*, 2004; *Lau and Kim*, 2007a; *Reale et al.*, 2014], while others found opposite effects [*Karyampudi and Carlson*, 1988; *Braun*, 2010]. Our study confirms the complexity of this subject. Radiatively active dust causes several effects in background conditions: (1) A low-level warming with a cooling above in the central SAL region, in agreement with *Wong et al.* [2009], *Wilcox et al.* [2010], and *Reale et al.* [2014]; (2) a drying of the atmosphere in this region; (3) an increase in vertical shear in large parts of the tropical North Atlantic; and (4) a strengthening of the vertical circulation associated with the AEJ. Results (1)–(3) confirm the findings of *Dunion and Velden* [2004] and (4) those of *Braun* [2010]. There is also a southward shift of convection within the ITCZ, but this shift is only small. Developing disturbances are shifted to the south by 1°, which is not statistically significant. For both types of disturbances no significant change in frequency can be determined. Changes in environmental conditions also depend on the optical properties of dust. An increase in dust absorption in the ECHAM6-Dust simulations would lead to a further warming of the SAL and stabilization of the atmosphere. Hence, subsequent increases in meridional and vertical motions presumably lead to an enhanced vertical circulation around the SAL.

On average, our DDs are located 4°–5° in latitude southward of the NDDs, due to the southward increasing SST west off the North African coastline. In addition, the northward increasing shear of 0 to 15 m s^{-1} between 10°N and 20°N is a crucial influencing factor for hurricane formation depending on its location. The large difference in dust burden between DDs and NDDs thus coincides with different average locations as the DDs are located mainly at the southern edge of the SAL.

We detect statistically significant changes in dust burden composites between ECHAM6-no-dust and ECHAM6-Dust simulations such that dust burden decreases for DDs in ECHAM6-Dust but increases for NDDs. However, neither shear nor vorticity reveal significant changes between ECHAM6-no-dust and ECHAM6-Dust. Accounting for the limitations in spatial resolution in our setup, this indicates that radiatively active dust does not have a significant impact on dynamical hurricane influential parameters during hurricane genesis. Changes in relative humidity also coincide with the variation in DD and NDD locations.

Variations in BDIs between ECHAM6-no-dust and ECHAM6-Dust do not show a pattern which could assign dust a crucial role. However, dust has a modulating effect due to changes in atmospheric stability as discussed above. In the study of *Peng et al.* [2012], thermodynamic variables (water vapor content, rain rate, and SST) have larger BDIs than dynamic variables (vorticity, vertical wind shear, and divergence) and are thus more important as hurricane genesis controlling variables. Even though we do not use all of these variables, we can reproduce this result with our model. A quantitative comparison of the BDIs with the variables from *Peng et al.* [2012] and ours is not feasible because of the different approaches of defining DDs and NDDs in the two studies. Although we also calculated BDIs for the 20° × 20° boxes as presented by *Peng et al.* [2012], uncertainties arise from our model resolution of 0.5° × 0.5°, which lead to a simulation of only low-intensity hurricanes that do not exceed category 1 on the Saffir/Simpson hurricane scale [*Simpson and Saffir*, 1974]. Additionally, our area of interest is different from *Peng et al.* [2012] (20°W–50°W versus 10°E–100°W in *Peng et al.* [2012]), which causes further inconsistencies.

One has to keep in mind that our findings are statistical results and do not exclude a potentially larger effect of dust and the SAL on individual storms. To assign (non)genesis and intensification of certain storms to the presence of dust and the SAL, these storms need to be examined carefully and individually as done by *Karyampudi and Pierce* [2002]. Furthermore, the too low spatial resolution in our simulations is a considerable constraint of our study. The results presented here only refer to systems of tropical storm intensity. However, the numbers in storms obtained by our TC-tracking algorithm are similar to long-term observations. Hence, we believe our results to be valid for a discussion about hurricane genesis and frequency. To evaluate intense storms as well, our method needs to be applied with significantly higher horizontal resolutions in a global or regional model. Besides resolution the second limitation of our study is the lack of atmosphere-ocean interactions in our model setup. We focused on the mechanisms suggested by *Dunion and Velden* [2004] but did not find any significant influence of dust on hurricane

genesis in our simulations. Using prescribed SSTs instead of interactive SSTs may lead to variations in regional circulation [*Miller et al.*, 2004]. Hence, for future studies we strongly recommend a coupled atmosphere-ocean model.

References

Bengtsson, L., K. I. Hodges, and M. Esch (2007a), Tropical cyclones in a T159 resolution global climate model: Comparison with observations and re-analyses, *Tellus A*, *59*, 316–416, doi:10.1111/j.1600-0870.2007.00236.x.

Bengtsson, L., K. I. Hodges, M. Esch, N. Keenlyside, L. Kornblueh, J.-J. Luo, and T. Yamagata (2007b), How may tropical cyclones change in a warmer climate?, *Tellus A*, *59*, 539–561, doi:10.1111/j.1600-0870.2007.00251.x.

Beven, J. L., L. A. Avila, E. S. Blake, D. P. Brown, J. L. Franklin, R. D. Knabb, R. J. Pasch, J. R. Rhome, and S. R. Stewart (2008), Atlantic hurricane season of 2005, *Mon. Weather Rev.*, *136*(3), 1109–1173, doi:10.1175/2007MWR2074.1.

Bracken, W. E., and L. F. Bosart (2000), The role of synoptic-scale flow during tropical cyclogenesis over the North Atlantic Ocean, *Mon. Weather Rev.*, *128*(2), 353–376.

Braun, S. A. (2010), Reevaluating the role of the Saharan air layer in Atlantic tropical cyclogenesis and evolution, *Mon. Weather Rev.*, *138*(6), 2007–2037, doi:10.1175/2009MWR3135.1.

Carlson, T. N., and J. M. Prospero (1972), The large-scale movement of Saharan air outbreaks over the northern equatorial Atlantic, *J. Appl. Meteorol.*, *11*(2), 283–297, doi:10.1175/1520-0450(1972)011<0283:TLSMOS>2.0.CO;2.

Carrio, G., and W. Cotton (2011), Investigations of aerosol impacts on hurricanes: Virtual seeding flights, *Atmos. Chem. Phys.*, *11*, 2557–2567, doi:10.5194/acp-11-2557-2011.

Cotton, W., H. Zhang, G. M. McFarquhar, and S. M. Saleeby (2007), Should we consider polluting hurricanes to reduce their intensity?, *J. Weather Modif.*, *39*, 70–73.

d'Almeida, G. A. (1986), A model for Saharan dust transport, *J. Clim. Appl. Meteorol.*, *25*(7), 903–916, doi:10.1175/1520-0450(1986)025<0903:AMFSDT>2.0.CO;2.

Dare, R. A., and J. L. McBride (2011), The threshold sea surface temperature condition for tropical cyclogenesis, *J. Clim.*, *24*(17), 4570–4576, doi:10.1175/JCLI-D-10-05006.1.

DeMott, P. J., K. Sassen, M. R. Poellot, D. Baumgardner, D. C. Rogers, S. D. Brooks, A. J. Prenni, and S. M. Kreidenweis (2003), African dust aerosols as atmospheric ice nuclei, *Geophys. Res. Lett.*, *30*(14), 1732, doi:10.1029/2003GL017410.

Dunion, J. P., and C. S. Velden (2004), The impact of the Saharan air layer on Atlantic tropical cyclone activity, *Bull. Am. Meteorol. Soc.*, *85*(3), 353–365, doi:10.1175/BAMS-85-3-353.

Evan, A. T., J. P. Dunion, J. A. Foley, A. K. Heidinger, and C. S. Velden (2006), New evidence for a relationship between Atlantic tropical cyclone activity and African dust outbreaks, *Geophys. Res. Lett.*, *33*, L19813, doi:10.1029/2006GL026408.

Foltz, G. R., and M. J. McPhaden (2008), Impact of Saharan dust on tropical North Atlantic SST*, *J. Clim.*, *21*(19), 5048–5060, doi:10.1175/2008JCLI2232.1.

Frank, N. L., and G. Clark (1980), Atlantic tropical systems of 1979, *Mon. Weather Rev.*, *108*(7), 966–972, doi:10.1175/1520-0493(1980)108>0966:ATSO>2.0.CO;2.

Frank, W. M., and P. E. Roundy (2006), The role of tropical waves in tropical cyclogenesis, *Mon. Weather Rev.*, *134*(9), 2397–2417, doi:10.1175/MWR3204.1.

Fu, B., M. S. Peng, T. Li, and D. E. Stevens (2012), Developing versus nondeveloping disturbances for tropical cyclone formation. Part II: Western North Pacific*, *Mon. Weather Rev.*, *140*(4), 1067–1080, doi:10.1175/2011MWR3618.1.

Gentry, R. C., and H. F. Hawkins (1970), A hypothesis for modification of hurricanes, *Project Stormfury Annual Rep. 1970*, U.S. Dep. Navy and U.S. Dep. of Commer., Washington, D. C.

Gray, W. (1998), The formation of tropical cyclones, *Meteorol. Atmos. Phys.*, *67*, 37–69, doi:10.1007/BF01277501.

Helmert, J., B. Heinold, I. Tegen, O. Hellmuth, and M. Wendisch (2007), On the direct and semidirect effects of Saharan dust over Europe: A modeling study, *J. Geophys. Res.*, *112*, D13208, doi:10.1029/2006JD007444.

Jones, C., N. Mahowald, and C. Luo (2003), The role of easterly waves on African desert dust transport, *J. Clim.*, *16*(22), 3617–3628, doi:10.1175/1520-0442(2003)016<3617:TROEWO>2.0.CO;2.

Karyampudi, V. M., and T. N. Carlson (1988), Analysis and numerical simulations of the Saharan air layer and its effect on easterly wave disturbances, *J. Atmos. Sci.*, *45*(21), 3102–3136, doi:10.1175/1520-0469(1988)045<3102:AANSOT>2.0.CO;2.

Karyampudi, V. M., and H. F. Pierce (2002), Synoptic-scale influence of the Saharan air layer on tropical cyclogenesis over the Eastern Atlantic, *Mon. Weather Rev.*, *130*(12), 3100–3128, doi:10.1175/1520-0493(2002)130<3100:SSIOTS>2.0.CO;2.

Khain, A., B. Lynn, and J. Dudhia (2010), Aerosol effects on intensity of landfalling hurricanes as seen from simulations with the WRF model with spectral bin microphysics, *J. Atmos. Sci.*, *67*, 365–384, doi:10.1175/2009JAS3210.1.

Kinne, S., et al. (2003), Monthly averages of aerosol properties: A global comparison among models, satellite data, and AERONET ground data, *J. Geophys. Res.*, *108*(D20), 4634, doi:10.1029/2001JD001253.

Kleppek, S., V. Muccione, C. C. Raible, D. N. Bresch, and P. S. T. Koellner-Heck (2008), Tropical cyclones in ERA-40: A detection and tracking method, *Geophys. Res. Lett.*, *35*, L10705, doi:10.1029/2008GL033880.

Krall, G., and W. Cottom (2012), Potential indirect effects of aerosol on tropical cyclone intensity: Convective fluxes and cold-pool activity, *Atmos. Chem. Phys. Discuss.*, *12*(1), 351–385, doi:10.5194/acpd-12-351-2012.

Kuettner, J. P. (1974), General description and central program of GATE, *Bull. Am. Meteorol. Soc.*, *55*(7), 712–719.

Landsea, C. W. (1993), A climatology of intense (or major) Atlantic hurricanes, *Mon. Weather Rev.*, *121*(6), 1703–1713, doi:10.1175/1520-0493(1993)121<1703:ACOIMA>2.0.CO;2.

Lau, W., and K. Kim (2007a), How nature foiled the 2006 hurricane forecasts, *Eos Trans. AGU*, *88*(9), 105–107, doi:10.1029/2007EO090002.

Lau, W., and K. Kim (2007b), Cooling of the Atlantic by Saharan dust, *Geophys. Res. Lett.*, *34*, L23811, doi:10.1029/2007GL031538.

Lighthill, J., G. Holland, W. M. Gray, C. W. Landsea, G. Craig, J. Evans, Y. Kurihara, and C. Guard (1994), Global climate change and tropical cyclones, *Bull. Am. Meteorol. Soc.*, *75*(11), 2147–2158.

Lim, Y.-K., S. D. Schubert, O. Reale, M.-I. Lee, A. M. Molod, and M. J. Suarez (2014), Sensitivity of tropical cyclones to parameterized convection in the NASA GEOS-5 model, *J. Clim.*, *28*, 551–573.

Martínez Avellaneda, N., N. Serra, P. Minnett, and D. Stammer (2010), Response of the eastern subtropical Atlantic SST to Saharan dust: A modeling and observational study, *J. Geophys. Res.*, *115*, C08015, doi:10.1029/2009JC005692.

Miller, R., J. Perlwitz, and I. Tegen (2004), Modeling Arabian dust mobilization during the Asian summer monsoon: The effect of prescribed versus calculated SST, *Geophys. Res. Lett.*, *31*, L22214, doi:10.1029/2004GL020669.

Molinari, J., D. Vollaro, and K. L. Corbosiero (2004), Tropical cyclone formation in a sheared environment: A case study, *J. Atmos. Sci.*, *61*(21), 2493–2509, doi:10.1175/JAS3291.1.

Murakami, H., and M. Sugi (2010), Effect of model resolution on tropical cyclone climate projections, *SOLA*, *6*, 73–76, doi:10.2151/sola.2010-019.

Murakami, H., et al. (2012), Future changes in tropical cyclone activity projected by the new high-resolution MRI-AGCM*, *J. Clim.*, *25*(9), 3237–3260, doi:10.1175/JCLI-D-11-00415.1.

Murakami, H., T. Li, and M. Peng (2013), Changes to environmental parameters that control tropical cyclone genesis under global warming, *Geophys. Res. Lett.*, *40*, 2265–2270, doi:10.1002/grl.50393.

Nolan, D. S., J. A. Zhang, and D. P. Stern (2009), Evaluation of planetary boundary layer parameterizations in tropical cyclones by comparison of in situ observations and high-resolution simulations of Hurricane Isabel (2003). Part I: Initialization, maximum winds, and the outer-core boundary layer, *Mon. Weather Rev.*, *137*(11), 3651–3674, doi:10.1175/2009MWR2785.1.

Nordeng, T. E. (1994), Extended versions of the convective parametrization scheme at ECMWF and their impact on the mean and transient activity of the model in the tropics, *Tech. Rep. 206*, European Center for Medium Range Weather Forecasts, Reading, England.

Peng, M. S., B. Fu, T. Li, and D. E. Stevens (2012), Developing versus nondeveloping disturbances for tropical cyclone formation. Part I: North Atlantic*, *Mon. Weather Rev.*, *140*(4), 1047–1066, doi:10.1175/2011MWR3617.1.

Prospero, J. M., and T. N. Carlson (1981), Saharan air outbreaks over the tropical North Atlantic, *Pure Appl. Geophys.*, *119*, 677–691, doi:10.1007/BF00878167.

Raible, C. C., S. Kleppek, M. Wueest, D. N. Bresch, A. Kitoh, H. Murakami, and T. F. Stocker (2012), Atlantic hurricanes and associated insurance loss potentials in future climate scenarios: Limitations of high-resolution AGCM simulations, *Tellus A*, *64*, 15672, doi:10.3402/tellusa.v64i0.15672.

Ramage, C. S. (1959), Hurricane development, *J. Meteorol.*, *16*(3), 227–237, doi:10.1175/1520-0469(1959)016<0227:HD>2.0.CO;2.

Reale, O., K. Lau, and A. da Silva (2011), Impact of interactive aerosol on the African easterly jet in the NASA GEOS-5 global forecasting system, *Weather Forecasting*, *26*(4), 504–519.

Reale, O., K. Lau, A. Silva, and T. Matsui (2014), Impact of assimilated and interactive aerosol on tropical cyclogenesis., *Geophys. Res. Lett.*, *41*(9), 3282–3288, doi:10.1002/2014GL059918.

Rosenfeld, D., M. Clavner, and R. Nirel (2011), Pollution and dust aerosols modulating tropical cyclones intensities, *Atmos. Res.*, *102*(1), 66–76, doi:10.1016/j.atmosres.2011.06.006.

Rosenfeld, D., W. L. Woodley, A. Khain, W. R. Cotton, G. Carrió, I. Ginis, and J. H. Golden (2012), Aerosol effects on microstructure and intensity of tropical cyclones, *Bull. Am. Meteorol. Soc.*, *93*(7), 987–1001, doi:10.1175/BAMS-D-11-00147.1.

Savtchenko, A., D. Ouzounov, S. Ahmad, J. Acker, G. Leptoukh, J. Koziana, and D. Nickless (2004), Terra and Aqua MODIS products available from NASA GES DAAC, *Adv. Space Res.*, *34*(4), 710–714.

Shao, Y., K.-H. Wyrwoll, A. Chappell, J. Huang, Z. Lin, G. H. McTainsh, M. Mikami, T. Y. Tanaka, X. Wang, and S. Yoon (2011), Dust cycle: An emerging core theme in Earth system science, *Aeolian Res.*, *2*(4), 181–204, doi:10.1016/j.aeolia.2011.02.001.

Simpson, R. H., and H. Saffir (1974), The hurricane disaster potential scale, *Weatherwise*, *27*(8), 169–186, doi:10.1080/00431672.1974.9931702.

Stanelle, T., I. Bey, T. Raddatz, C. Reick, and I. Tegen (2014), Anthropogenically induced changes in twentieth century mineral dust burden and the associated impact on radiative forcing, *J. Geophys. Res. Atmos.*, *119*, 13,526–13,546, doi:10.1002/2014JD022062.

Stevens, B., et al. (2013), The atmospheric component of the MPI-M Earth system model: ECHAM6, *J. Adv. Model. Earth Syst.*, *5*, 146–172, doi:10.1002/jame.20015.

Stier, P., et al. (2005), The aerosol-climate model ECHAM5-HAM, *Atmos. Chem. Phys.*, *5*, 1125–1156, doi:10.5194/acp-5-1125-2005.

Strachan, J., P. L. Vidale, K. Hodges, M. Roberts, and M.-E. Demory (2013), Investigating global tropical cyclone activity with a hierarchy of AGCMs: The role of model resolution, *J. Clim.*, *26*(1), 133–152, doi:10.1175/JCLI-D-12-00012.1.

Sun, D., K. Lau, and M. Kafatos (2008), Contrasting the 2007 and 2005 hurricane seasons: Evidence of possible impacts of Saharan dry air and dust on tropical cyclone activity in the Atlantic basin, *Geophys. Res. Lett.*, *35*, L15405, doi:10.1029/2008GL034529.

Tegen, I., and A. A. Lacis (1996), Modeling of particle size distribution and its influence on the radiative properties of mineral dust aerosol, *J. Geophys. Res.*, *101*(D14), 19,237–19,244, doi:10.1029/95JD03610.

Tegen, I., S. P. Harrison, K. Kohfeld, I. C. Prentice, M. Coe, and M. Heimann (2002), Impact of vegetation and preferential source areas on global dust aerosol: Results from a model study, *J. Geophys. Res.*, *107*(D21), 4576–4597, doi:10.1029/2001JD000963.

Tiedtke, M. (1989), A comprehensive mass flux scheme for cumulus parameterization in large-scale models, *Mon. Weather Rev.*, *117*(8), 1779–1800, doi:10.1175/1520-0493(1989)117<1779:ACMFSF>2.0.CO;2.

Tory, K. J., and W. M. Frank (2010), Tropical cyclone formation, in *Global Perspectives On Tropical Cyclones: From Science to Mitigation*, edited by J. C. L. Chan and J. D. Kepert, chap. 2, pp. 55–92, World Sci., Singapore.

Vamborg, F., V. Brovkin, and M. Claussen (2014), Background albedo dynamics improve simulated precipitation variability in the Sahel region., *Earth Syst. Dynam.*, *5*, 89–101, doi:10.5194/esd-5-89-2014.

van den Heever, S. C., G. G. Carrió, W. R. Cotton, P. J. DeMott, and A. J. Prenni (2006), Impacts of nucleating aerosol on Florida storms. Part I: Mesoscale simulations, *J. Atmos. Sci.*, *63*(7), 1752–1775, doi:10.1175/JAS3713.1.

Wang, Y., K.-H. Lee, Y. Lin, M. Levy, and R. Zhang (2014), Distinct effects of anthropogenic aerosols on tropical cyclones, *Nat. Clim. Change*, *4*, 368–373, doi:10.1038/nclimate2144.

Washington, R., M. Todd, N. J. Middleton, and A. S. Goudie (2003), Dust-storm source areas determined by the total ozone monitoring spectrometer and surface observations, *Ann. Assoc. Am. Geogr.*, *93*(2), 297–313, doi:10.1111/1467-8306.9302003.

Wilcox, E. M., K. Lau, and K.-M. Kim (2010), A northward shift of the North Atlantic Ocean Intertropical Convergence Zone in response to summertime Saharan dust outbreaks, *Geophys. Res. Lett.*, *37*, L04804, doi:10.1029/2009GL041774.

Willoughby, H., D. Jorgensen, R. Black, and S. Rosenthal (1985), Project STORMFURY: A scientific chronicle 1962–1983, *Bull. Am. Meteorol. Soc.*, *66*(5), 505–514.

Wong, S., A. E. Dessler, N. M. Mahowald, P. Yang, and Q. Feng (2009), Maintenance of lower tropospheric temperature inversion in the Saharan air layer by dust and dry anomaly, *J. Clim.*, *22*(19), 5149–5162, doi:10.1175/2009JCLI2847.1.

Woodage, M., and S. Woodward (2014), UK HiGEM: Impacts of desert dust radiative forcing in a high-resolution atmospheric GCM, *J. Clim.*, *27*, 5907–5928.

Zarzycki, C. M., and C. Jablonowski (2014), A multidecadal simulation of Atlantic tropical cyclones using a variable-resolution global atmospheric general circulation model, *J. Adv. Model. Earth Syst.*, *6*(3), 805–828.

Zhang, H., G. McFarquhar, S. Saleeby, and W. Cotton (2007), Impacts of Saharan dust as CCN on the evolution of an idealized tropical cyclone, *Geophys. Res. Lett.*, *34*, L14812, doi:10.1029/2007GL029876.

Zhang, H., G. M. McFarquhar, W. Cotton, and Y. Deng (2009), Direct and indirect impacts of Saharan dust acting as cloud condensation nuclei on tropical cyclone eyewall development, *Geophys. Res. Lett.*, *36*, L06802, doi:10.1029/2009GL037276.

Zhang, K., et al. (2012), The global aerosol-climate model ECHAM-HAM, version 2: Sensitivity to improvements in process representations, *Atmos. Chem. Phys.*, *12*(19), 8911–8949, doi:10.5194/acp-12-8911-2012.